

# Enhancing absorption efficiency by incorporating hollow titanium particles in perovskite solar cells

Ziyu Chen\*, Yingzi Wang, Huiming Shen

Wuhan Electric Power Technical College, Wuhan 430079 China

\*Corresponding author, e-mail: ziyu\_chen\_whetc11@foxmail.com

Received 3 Apr 2024, Accepted 30 May 2025

Available online 29 Jun 2025

**ABSTRACT:** Since the advent of hybrid metal halide perovskite as an exceptional light-absorbing material, it has achieved remarkable advancements in enhancing the efficiency of solar cells. Building upon this foundation, the reconstruction of the internal optical properties of perovskite is anticipated to improve its efficiency further. To this end, we have investigated the impact of hollow metallic titanium particle structures on absorption rates and discovered that incorporating hollow metallic titanium structures into perovskite thin films can further enhance absorption rates compared to gold and silver nanoparticles. Ultimately, through comparative testing, we found that the solar spectral absorption rate of perovskite thin-film photovoltaic cells with a single-layer thickness of 200 nm was increased by 32%.

**KEYWORDS:** perovskite, Ti particles, nanostructures, solar cells, absorption rate

## INTRODUCTION

Since the emergence of perovskite solar cells (PSCs) [1, 2], they have attracted considerable attention across various research domains [3–5]. The distinctive optoelectronic characteristics of perovskite ( $\text{CH}_3\text{NH}_3\text{PbI}_3$ ), including its direct bandgap, high absorption coefficient, low exciton binding energy, tunable bandgap, long carrier diffusion length, and straightforward fabrication processes, have fueled rapid advancements over the past decade [6]. From 2009 to 2021, the power conversion efficiency (PCE) of PSCs has surged from 3.8% to over 24% [7, 8]. However, the primary focus of researchers has been on enhancing its optoelectronic performance and addressing material stability concerns. A significant barrier to widespread adoption is the high manufacturing cost, leading to the production and measurement of thin layers to mitigate expenses [9, 10]. Nevertheless, effective photon management is crucial for achieving optimal performance. Plasmonic nanostructures offer promise in concentrating [11] and enhancing the local electric field [12–15]. Exhibited by metal nanostructures [16–19] or metal-oxide nanostructures [20, 21], the localized surface plasmon resonance (LSPR) effect holds incredible potential [22–25]. To further enhance the performance of perovskite photovoltaic cells [26–28], leveraging the LSPR effect to increase light absorption has proven highly effective [29, 30], gold, silver, and aluminum nanostructures show an outstanding effect [31, 32]. However, titanium and its oxides also exhibit outstanding absorption enhancement effects at the nanoscale [33]. This structure enhances the absorption spectrum of PSCs in the visible light region through the LSPR effect and near-field scattering. The absorption enhancement factor  $\eta$  under different conditions was precisely calculated using Finite Difference Time Domain (FDTD) simulations,

which illustrate the promising prospects of this design for improving the capability of solar light collection.

## MATERIALS AND METHODS

Investigations into the solar absorption characteristics of perovskite films with embedded metal nanostructures of various shapes were conducted using the FDTD simulation method. To achieve high precision and stable results, a dense grid with a refined minimum of 1 nm was utilized. The perovskite film, interposed between spiro-OMeTAD and a  $\text{TiO}_2$  glass substrate, was modeled with photovoltaic parameters and material optical constants derived from previous work [34]. The simulation employed plane wave sources with the default polarization aligned along the X-axis.

The baseline transmittance and reflectance of the unadulterated perovskite film structure were measured, and a reference absorption rate,  $\alpha_{\text{ref}}$ , was established using the equation  $\alpha = 1 - R - T$ . The enhancement factor of the absorption rate, denoted as  $\eta(\lambda)$ , was then calculated by dividing the absorption rate with the inclusion of metal nanostructures by the reference value, thus  $\eta(\lambda) = \alpha_p / \alpha_{\text{ref}}$ .

The visible light range absorption rate enhancement factor  $\eta$ , is formulated as

$$\eta = \frac{\int_{300}^{800} \alpha_p(\lambda) \text{AM1.5} d\lambda}{\int_{300}^{800} \alpha_{\text{ref}}(\lambda) \text{AM1.5} d\lambda} \quad (1)$$

with AM1.5 representing the solar spectrum after atmospheric passage. From previous report [34], simulations using the SCAPS software revealed that the short-circuit current density  $J_{\text{sc}}$  for the modeled perovskite photovoltaic cell is  $19.38 \text{ mA/cm}^2$ , yielding an energy conversion efficiency (PCE) of 17.85%. Prior research [32] has indicated that aluminum exhibits an absorption peak more aligned with the visible light spectrum

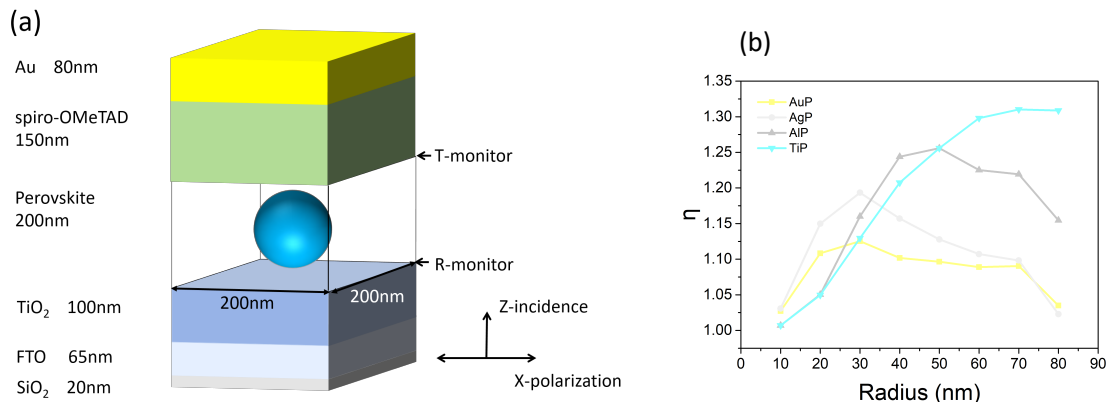


**Fig. 1** (a) A practical-oriented model of a perovskite photovoltaic cell and the dimensions of the parts, with the transmission and reflection observation windows set on both sides of the perovskite. (b) The relationship between the enhancement of absorption rate and the particle radius when adding gold, silver, aluminum, and titanium at the center of the perovskite thin film.

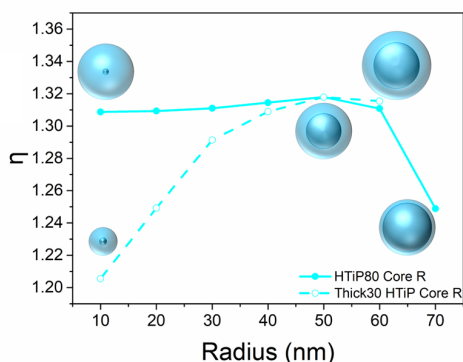


**Fig. 2** The solid line represents the relationship between the absorption enhancement factor  $\eta$  and the inner diameter as the core within the HTiP of 80 nm radius is gradually increased. The dashed line illustrates the relationship between  $\eta$  and the gradually increasing inner diameter when the difference between the outer and inner diameters is fixed at 30 nm.

when compared to gold and silver, and its production cost is significantly lower.

## RESULTS AND DISCUSSION

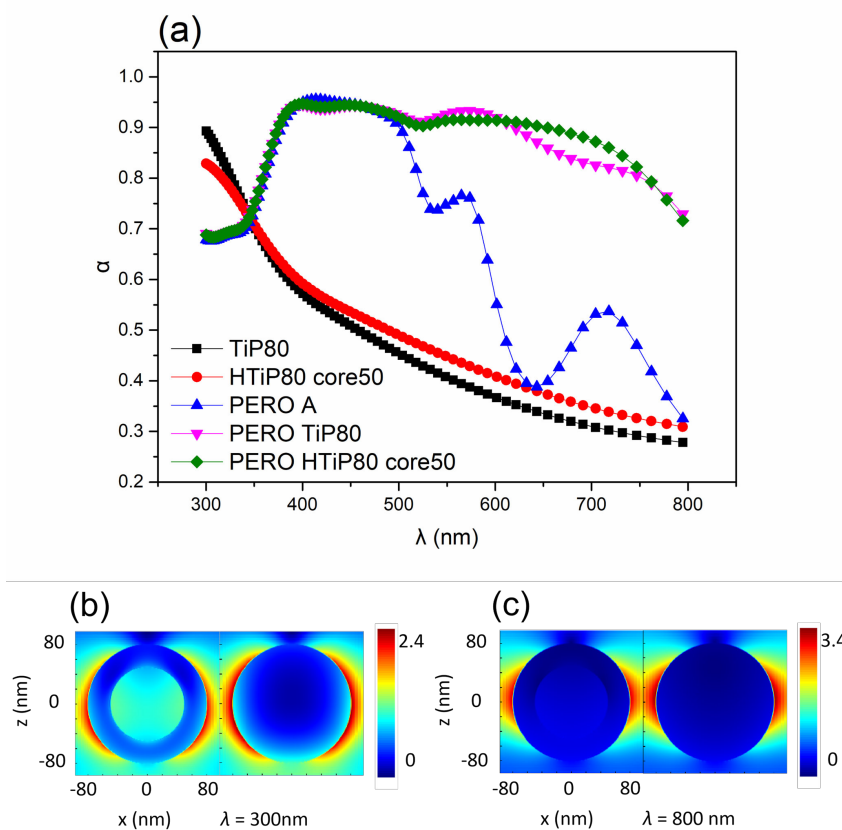
From Fig. 1, it can be observed that both gold and silver achieve the maximum enhancement at a radius of 30 nm, while the aluminum particles (AlP) exhibit their maximum enhancement at a radius of 50 nm, with the perovskite section measuring  $200 \times 200 \times 200$  nm. The titanium particles (TiP) show the greatest enhancement effect within the radius range of 70–80 nm. Interestingly, the use of TiP doping resulted in an unexpectedly better outcome compared to gold, silver, and aluminum. Given that hollow metallic aluminum

can produce superior absorption enhancement effects, it is reasonable to expect that hollow metallic titanium would also exhibit a similar effect.

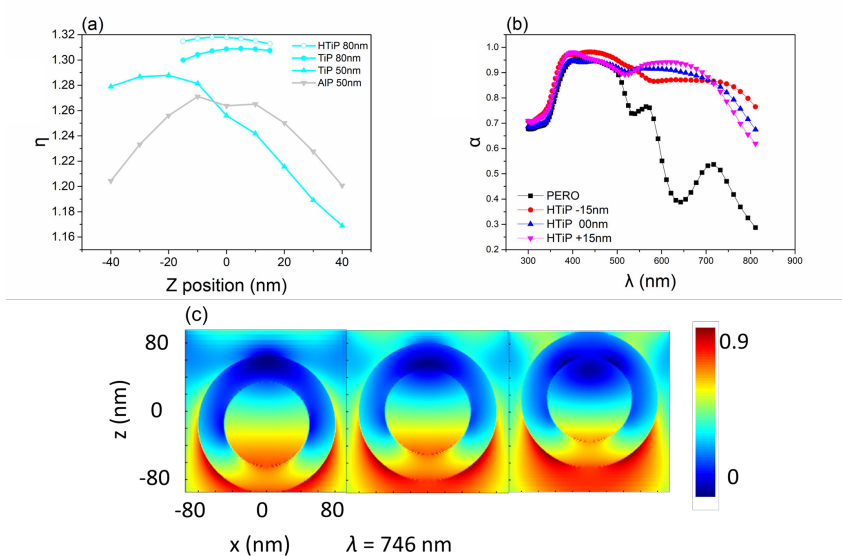
The following result showed that the introduction of a hollow core can further enhance the absorption enhancement effect of TiP (Fig. 2). When the core radius reaches 50 nm, the absorption enhancement factor  $\eta$  reaches its peak at 31.8%. Similarly, when the thickness of the hollow titanium particle (HTiP) is fixed at 30 nm and the core radius is increased, the  $\eta$  value also peaks at 31.8% at a core radius of 50 nm before declining. According to our previous work [35], the improvement in absorption enhancement by adding a core to AlP is essentially an effect of the HAIP structure itself, rather than the material of the core. The incident light passes through the thinner shell and induces a secondary LSPR and scattering effect at the inner surface of the HTiP.

Fig. 3(a) demonstrated that compared to TiP with the same outer diameter, HTiP with a thin metal layer of only 30 nm significantly enhances absorption across most of the spectral range, outperforming solid nanoparticles. Both TiP and HTiP notably improve the absorption rate in the lower absorption region of perovskite between 500 nm~800 nm, positioning the absorption rate largely within the higher range of 0.8 to 0.9, thereby enhancing the overall absorption rate. This is more intuitively reflected in the electric field intensity distribution diagrams of Fig. 3(b,c) that the core looks hard to be ignored. According to the previous work [18], the optimal position for AuP to achieve the best absorption enhancement in PSCs is at the center of the perovskite layer. However, the characteristics of TiP and HTiP may differ due to the additional inner LSPR, which could alter the effect.

For AuP, the LSPR near-field effect plays a primary role when close to the direction of incident light,



**Fig. 3** (a) The relationship between the absorption rate  $\alpha$  and wavelength for HTiP with a thickness of 30 nm and an outer diameter of 80 nm, compared to TiP of the same dimensions. (b, c) The electric field distribution of HTiP and TiP at wavelengths of 300 nm and 800 nm, respectively.



**Fig. 4** (a) The relationship between  $\eta$  and the Z-axis position for metal nanoparticles with different outer diameters, where 0 represents the center of the PSC film, and the direction of light incidence ranges from negative to positive. (b) The relationship between the absorption rate  $\alpha$  and the Z-axis position for HTiP with an outer diameter of 50 nm. (c) The electric field distribution of HTiP at a wavelength of 746 nm as the Z-axis position changes.

while scattering dominates when further away from the light source [18]. At intermediate positions, the combined effects of near-field and scattering lead to the optimal absorption enhancement, a characteristic that Al shares with Au, as reproduced in Fig. 4(a). However, it can also be observed from this figure that for TiP with an outer diameter of 50 nm, the absorption enhancement factor  $\eta$  does not decrease but instead increases in the half-space close to the direction of incident light. At positions between  $-20$  nm and  $-30$  nm, the absorption enhancement can reach over 28%. In the half-space away from the incident light, the trend is similar to that of AlP.

When the outer diameter of TiP reaches 80 nm, not only does  $\eta$  continue to increase, but the influence of the Z-axis position becomes negligible, which is also true for HTiP. This is evident in Fig. 4(b), where the absorption rate within the spectral range of 600 nm–700 nm and 700 nm–800 nm forms a compensatory effect due to distance changes, offsetting the variations in  $\eta$  value caused by distance. The electric field intensity map in Fig. 4(c) also demonstrates this point. Due to the presence of an inner surface in HTiP and HAIP, the near-field effect is significantly enhanced [35], while the scattering effect is considerably weakened. This results in HTiP not achieving the maximum enhancement effect at the center of the PSC but rather at positions biased towards the direction of incident light. With an outer diameter increased to 80 nm, HTiP's proximity to the incident light direction shortens, making the near-field effect predominant.

From the perspective of absorption rate, the addition of HTiP to perovskite stabilizes the overall absorption rate within the visible light range at 0.8 to 0.9, enabling a more effective and balanced solar energy absorption compared to the aforementioned HAIP. The corresponding  $J_{sc}$  calculated is approximately 25.58%, surpassing the reported world record [36].

## CONCLUSION

It has been demonstrated that the use of TiP in perovskite solar cells can enhance their absorption rate by 25%, outperforming gold, silver, and aluminum. The incorporation of a core to form HTiP can further increase the absorption rate to approximately 32%, like HAIP. FDTD numerical simulation results indicate that the enhancement of light absorption is due to the excitation of LSPR modes, the near-field effect of the nanostructures, and backscattering. The addition of an inner surface and the larger outer diameter contribute significantly to the gain in the near-field effect. The insensitivity to the Z-axis position also implies less stringent requirements for the fabrication process of PSCs, thereby achieving more efficient perovskite solar cells.

**Acknowledgements:** The authors would like to express their sincere gratitude to the Research Office of our affiliated

college for providing the necessary research facilities and resources. Their support was instrumental in creating an environment conducive to academic exploration and research.

## REFERENCES

1. Lee MM, Teuscher J, Miyasaka T, Murakami TN, Snaith HJ (2012) Efficient hybrid solar cells based on meso-structured organometal halide perovskites. *Science* **338**, 643.
2. Green MA, Ho-Baillie A, Snaith HJ (2014) The emergence of perovskite solar cells. *Nat Photonics* **8**, 506–514.
3. Shi D, Adinolfi V, Comin R, Yuan M, Alarousu E, Buin A, Chen Y, Hoogland S, et al (2015) Low trap state density and long carrier diffusion in organolead trihalide perovskite single crystals. *Science* **347**, 519–522.
4. Grätzel M (2014) The light and shade of perovskite solar cells. *Nat Mater* **13**, 838–842.
5. Tan Z-K, Moghaddam RS, Lai MLL, Docampo P, Higler R, Deschler F, Price M, Sadhanala A, et al (2014) Bright light-emitting diodes based on organometal halide perovskite. *Nat Nanotechnol* **9**, 687–692.
6. Shamsi J, Urban AS, Imran M, De Trizio L, Manna L (2019) Metal halide perovskite nanocrystals: synthesis, post-synthesis modifications, and their optical properties. *Chem Rev* **119**, 3296–3348.
7. Kojima A, Teshima K, Shirai Y, Miyasaka T (2009) Organometal halide perovskites as visible-light sensitizers for photovoltaic cells. *J Am Chem Soc* **131**, 6050–6051.
8. Jeong M, Choi IW, Go EM, Cho Y, Kim B, Lee S, Jeong Y, Jo H, et al (2020) Stable perovskite solar cells with efficiency exceeding 24.8% and 0.3-V voltage loss. *Science* **369**, 1615–1620.
9. Usman A, Jiraraksopakun Y, Kaewon R, Pawong C, Bhatranand A (2022) The comparison of multi-stepping algorithms for real-time thickness measurement of transparent thin films using polarization settings. *Laser Physics* **32**, 125401.
10. Usman A, Bhatranand A, Jiraraksopakun Y, Kaewon R, Pawong C (2021) Real-time double-layer thin film thickness measurements using modified Sagnac interferometer with polarization phase shifting approach. *Photonics* **8**, 529.
11. Knight MW, Sobhani H, Nordlander P, Halas NJ (2011) Photodetection with active optical antennas. *Science* **332**, 702–704.
12. Akimov AV, Mukherjee A, Yu CL, Chang DE, Zibrov AS, Hemmer PR, Park H, Lukin MD (2007) Generation of single optical plasmons in metallic nanowires coupled to quantum dots. *Nature* **450**, 402–406.
13. Zhou ZK, Li M, Yang ZJ, Peng XN, Su XR, Zhang JB, Li NC, Kim XF, et al (2010) Plasmon-mediated radiative energy transfer across a silver nanowire array via resonant transmission and subwavelength imaging. *ACS Nano* **4**, 5003–5010.
14. Sorger VJ, Zhang X (2011) Physics. Spotlight on plasmon lasers. *Science* **333**, 709–710.
15. Fan JA, Wu C, Bao K, Bao J, Bardhan R, Halas NJ, Manoharan VN, Nordlander P, et al (2010) Self-assembled plasmonic nanoparticle clusters. *Science* **328**, 1135–1138.

16. Zhang W, Anaya M, Lozano G, Calvo ME, Johnston H, Míguez H, Snaith HJ (2015) Highly efficient perovskite solar cells with tunable structural color. *Nano Lett* **15**, 1698–1702.
17. Tavakoli MM, Tsui K-H, Zhang Q, He J, Yao Y, Li D, Fan Z (2015) Highly efficient flexible perovskite solar cells with antireflection and self-cleaning nanostructures. *ACS Nano* **9**, 10287–10295.
18. Carretero-Palacios S, Calvo ME, Míguez H (2015) Absorption enhancement in organic-inorganic halide perovskite films with embedded plasmonic gold nanoparticles. *J Phys Chem C* **119**, 18635–18640.
19. Carretero-Palacios S, Jimenez-Solano A, Míguez H (2016) Plasmonic nanoparticles as light-harvesting enhancers in perovskite solar cells: A user's guide. *ACS Energy Lett* **1**, 323–331.
20. Han SC, Cui LL, Li ZW, Luan K (2024) High energy storage performance of  $(1-x)\text{Ba}_{0.9}\text{Ca}_{0.1}\text{TiO}_3-x\text{BaSn}_{0.1}\text{Ti}_{0.9}\text{O}_3$  bulk ceramics. *ScienceAsia* **50**, ID 2024092.
21. Wang SF, Tong YJ (2023) Investigation on sensitivity of photo-thermal conversion efficiency of an enclosed type evacuated U-tube solar collector using  $\text{Fe}_3\text{O}_4$ -MWCNT/water hybrid nanofluid. *ScienceAsia* **50**, ID 2024017.
22. Kong D, Xu J, Zhan R, Duan X, Zhou ZK (2016) Surface plasmon-enhanced third-order optical non-linearity of silver triangular nanoplate. *J Mod Opt* **63**, 2396.
23. Yu Y, Ji Z, Zu S, Du B, Kang Z, Li Z, Zhou K, Shi Z, et al (2016) Ultrafast plasmonic hot electron transfer in Au nanoantenna/ $\text{MoS}_2$  heterostructures. *Adv Funct Mater* **26**, 6394.
24. Zhang W, Saliba M, Stranks S, Sun Y, Shi X, Wiesner U, Snaith HJ (2013) Enhancement of perovskite based solar cells employing core-shell metal nanoparticles. *Nano Lett* **13**, 4505–4510.
25. Yuan Z, Wu Z, Bai Z, Xia W, Xu T, Song H, Wu L, Xu J, et al (2015) Hot-electron injection in a sandwiched  $\text{TiO}_x$ -Au- $\text{TiO}_c$  structure for high-performance planar perovskite solar cells. *Adv Energy Mater* **5**, 1500038.
26. Lu Z, Pan Y, Ma Y, Li L, Zheng D, Zhang Q, Xu Z, Chen S, et al (2015) Plasmonic-enhanced perovskite solar cells using alloy popcorn nanoparticles. *RSC Adv* **5**, 11175–11179.
27. Hsu H, Juang T, Chen C, Hsieh C, Yang C, Huang C, Jeng R (2015) Enhanced efficiency of organic and perovskite photovoltaics from shape-dependent broadband plasmonic effects of silver nanoplates. *Sol Energy Mater Sol Cells* **140**, 224–231.
28. Wang G, Meng ZH, He L, Wu ZH, Liu X, Wang W, Li R, Tai SH, et al (2017) Wide-angle polarization-free plasmon enhanced light absorption in perovskite films using silver nanowires. *Opt Express* **25**, 4.
29. Tooghi A, Fathi D, Eskandari, M (2020) High-performance perovskite solar cell using photonic-plasmonic nanostructure. *Sci Rep* **10**, 11248.
30. Yue L, Yan B, Attridge M, Wang Z (2016) Light absorption in perovskite solar cell: Fundamentals and plasmonic enhancement of infrared band absorption. *Sol Energy* **124**, 143–152.
31. Chen Z, Li X, Guo X (2023) Enhanced absorption in perovskite solar cells by incorporating gold triangle nanostructures. *Appl Opt* **62**, 5064–5068.
32. Chen Z, Li X, Chen C (2024) Enhancement of absorption by incorporating aluminum triangular nanostructures into perovskite. *J Nanophotonics* **18**, 016004.
33. Xu M, Zhu X, Shi J, Liang Y, Jin Y, Wang Z, Liao L (2013) Plasmon resonance enhanced optical absorption in inverted polymer/fullerene solar cells with metal nanoparticle-doped solution-processable  $\text{TiO}_2$  layer. *ACS Appl Mater Interfaces* **5**, 2935–2942.
34. Jangjoy A, Matloub S (2023) Theoretical study of Ag and Au triple core-shell spherical plasmonic nanoparticles in ultra-thin film perovskite solar cells. *Opt Express* **31**, 19102–19115.
35. Chen Z, Chen C, Chen P (2024) Enhancing absorption rate in perovskite by incorporating hollow nano aluminum particles. *Sci Adv Mater* **16**, 1–5.
36. Gao H, Xiao K, Lin RX, Zhao SY, Wang WL, Dayneko S, Duan CY, Ji CL, et al (2024) Homogeneous crystallization and buried interface passivation for perovskite tandem solar modules. *Science* **383**, 855–859.